ELSEVIER

Journal of Marine Systems 36 (2002) 173–196

JOURNAL OF MARINE SYSTEMS

www.elsevier.com/locate/jmarsys

Modelling the spatial and temporal variability of the Cretan Sea ecosystem

George Petihakis[a,*], George Triantafyllou[a], Icarus J. Allen[b], Ibrahim Hoteit[c], Costas Dounas[a]

[a] *Institute of Marine Biology of Crete, P.O. Box 2214, Iraklio 71003, Crete, Greece*
[b] *Plymouth Marine Laboratory, Prospect Place, West Hoe, Plymouth PL1 3DH, UK*
[c] *Laboratoire de Modelisation et calcul, Tour IRMA BP 53, Grenoble cedex 9 F-38041, France*

Received 28 May 2001; accepted 17 April 2002

Abstract

The ecosystem function of the oligotrophic Cretan Sea is explored through the development and application of a 3D ecological model. The simulation system comprises of two on-line coupled submodels: the 3D Princeton Ocean Model (POM) and the 1D European Regional Seas Ecosystem Model (ERSEM) adapted to the Cretan Sea. For the tuning and initialisation of the ecosystem parameters, the 1D version of the biogeochemical model is used.

After a model spin up period of 10 years to reach a quasi-steady state, the results from an annual simulation are presented. A cost function is used as validation method for the comparison of model results with field data. The estimated annual primary and bacteria production are found to be in the range of the reported values. Simulation results are in good agreement with in situ data illustrating the role of the physical processes in determining the evolution and variability of the ecosystem.

Keywords: 3D ecosystem model; Oligotrophic ecosystem; Cretan Sea

1. Introduction

The Cretan Sea is the largest and deepest basin (2500 m) in the south Aegean Sea. It has an average depth of 1000 m and two deeper troughs in the eastern part (2561 and 2295 m). It is linked with the Levantine basin and the Ionian Sea through the eastern and western straits of the Cretan Arc, respectively, via sills that are no deeper than 700 m. Outside the straits, the seabed plunges towards the deep basins of the Hellenic Trench (depth ~ 3000–4000 m). To the north, it is bounded by the Cyclades Plateau at a depth of 600 m (Fig. 1).

The hydrological structure in the Cretan Sea is dominated by multiple-scale circulation patterns and is an area of deep-water formation. It acts as a reservoir for heat and salt for the Eastern Mediterranean, and is characterised by intense mesoscale activity (Georgopoulos et al., 2000), which is not necessarily seasonally driven. The circulation in the Cretan Sea is dictated by the combined effect of two gyral features: an anticyclonic eddy in the west and a cyclonic eddy in the east (Georgopoulos et al., 2000;

* Corresponding author. Tel.: +30-81-346-860; fax: +30-81-241-882.

0924-7963/02/$ - see front matter © 2002 Elsevier Science B.V. All rights reserved.
PII: S0924-7963(02)00186-0

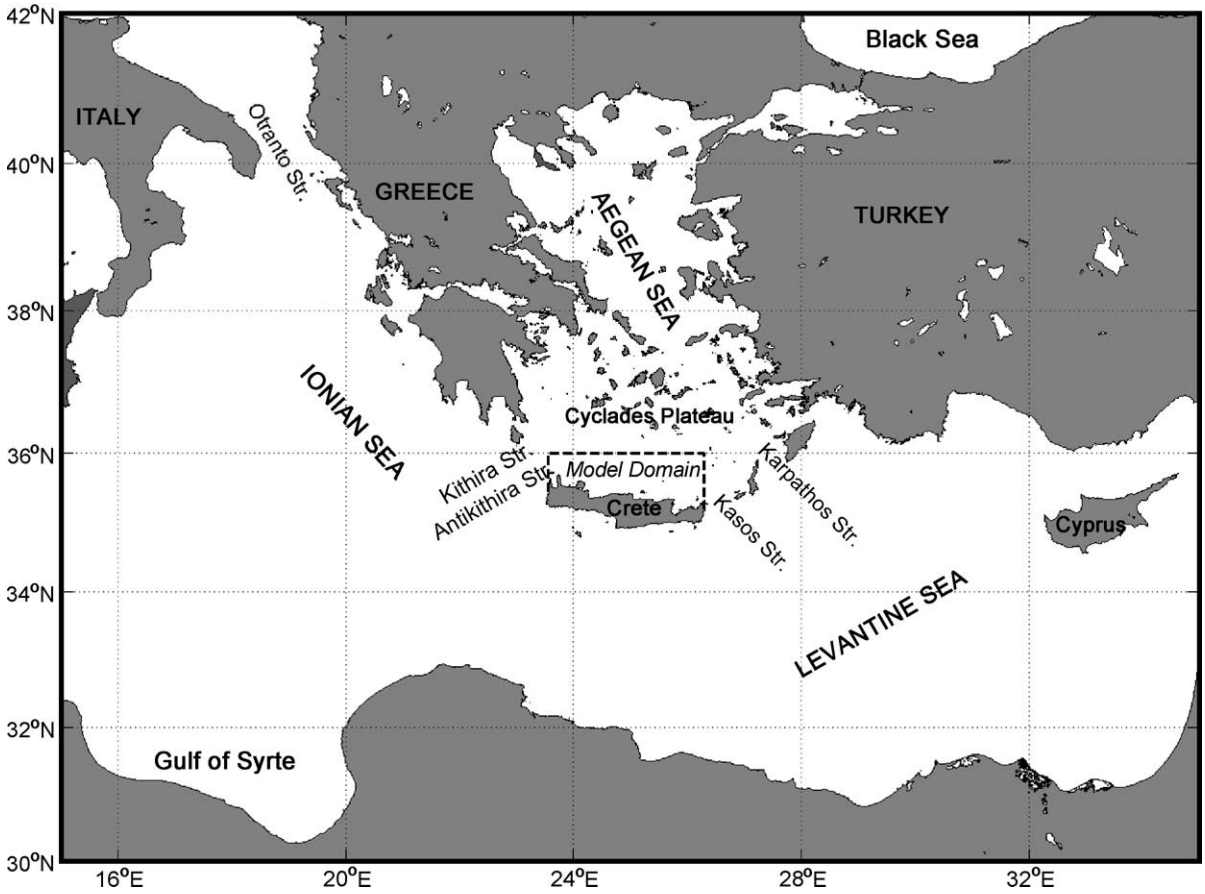

Fig. 1. Map of the Eastern Mediterranean and model domain.

Theocharis et al., 1999). The surface waters are dominated by Modified Atlantic Waters (MAW). Beneath the MAW lies the Cretan Intermediate Water (CIW) and the Transient Mediterranean Water (TMW), which is a very important water mass characterised by low temperature (14 °C) and salinity (38.7 psu) intruding into the Cretan Sea via the eastern Kassos and western Antikithira straits occupying the intermediate layer 200–600 m (Balopoulos et al., 1999). The presence of the TMW is rather variable and is associated with the outflow of Cretan Deep Water (CDP) into the eastern Mediterranean (Souvermezoglou et al., 1999). Since TMW is old water, it is characterised by high-nutrient and low-oxygen concentrations. Nutrient concentrations in this layer are the highest measured with an increase in nitrates by 2.5 μM, of phosphates by 0.05 μM and of silicates by 2.5 μM, and, conversely, a remarkable decrease of oxygen concentrations reaching 0.8 ml/l (35 μM) (Souvermezoglou et al., 1999). In late winter, the intensity of the eddy dipole in the Cretan Sea increases and the TMW downwells in the west of the domain (to 500–900 m) and upwells at the center of the cyclone (from 20 to 600 m). This upwelling of nutrients into the euphotic zone can be very important ecologically as it initiates small-scale phytoplankton blooms. During spring, summer and autumn, the Cretan Sea is stratified and exhibits an oligotrophic ecosystem characterized by a food chain composed of very small phytoplankton cells and a microbial loop, both of which have a negative effect on energy transfer (carbon and nutrients) to the deeper water layers and the benthos. This is magnified by the high water temperatures (>14 °C) and high oxygen concentra-

tions (>4 ml l^{-1}) enhancing decomposition rates of organic matter leaching out from the euphotic zone. The very low nutrient concentrations found in the Eastern Mediterranean, in conjunction with the prevailing hydrographic circulatory patterns, are the main factors responsible for maintaining low-phytoplankton standing stock and surface primary production levels observed (Azov, 1986; Becacos-Kontos, 1977; Berman et al., 1984).

In early spring, intense mixing occurs and the euphotic zone is resupplied with nutrients from deep waters. Even so, phytoplankton biomass remains at relatively low levels due to phosphate limitation. Phosphate in the Mediterranean Sea is considered as the main nutrient limiting factor of phytoplankton (Becacos-Kontos, 1977; Berland et al., 1980; Krom et al., 1991; Thingstad and Rassoulzadegan, 1995), with the concentrations decreasing from west to east. Small cells dominate the euphotic zone during stratification because concentrations of nutrients in particular phosphate are near detection limit and must be recycled at a high rate and, therefore, cells of small size are competitively superior relative to larger cells. During stratification, the microbial loop dominates the pelagic food web (DOC–bacteria–protozoa), and unicellular organisms are responsible for almost the entire energy flow and mineralization processes in the water column restricting energy transfer to deeper layers. During mixing (winter–early spring), the system adopts a more traditional type of food chain with diatoms dominating and sedimentation is maximized. Deep mixing is responsible for phytoplankton transfer to deep waters refuelling benthos with nutritious material. Fluctuations in biogeochemical components in the Cretan Sea can be interannual. It periodically undergoes periods of high nutrient availability due to intense mixing, which may cause dramatic changes in the productivity of the area. When this occurs, the entire system responds by shifting its food web structure from the microbial type to the classical type, which generates larger sedimenting particles and, therefore, increases energy transfer to the deeper water layers and the benthos.

In spite of the importance and the favourable position of the Mediterranean Sea, it is only recently that numerical studies of the ecosystem have been carried out. Most work primarily focused on the development and application of 1D models at the Western and Central Mediterranean (Allen et al., 1998; Klein and Coste, 1984; Solidoro et al., 1998; Tusseau et al., 1997; Varela et al., 1992; Zakardjian and Prieur, 1994), while fully 3D models have been developed for larger but still limited areas at the same wider region (Bergamasco et al., 1998; Civitarese et al., 1996; Levy et al., 1998; Pinazo et al., 1996; Tusseau et al., 1997; Zavatarelli et al., 2000). A model for the whole Mediterranean ecosystem (Crise et al., 1999) uses a very simplified ecosystem structure focusing upon nitrogen cycling rather than biological organisms. In the case of Cretan Sea ecosystem, the 1D complex model developed and applied successfully (Triantafyllou et al., 2002b) is used for the development of the fully 3D model presented in this paper. This attempt is innovative since it combines two complex models fully describing both physical and biological domains of the oligotrophic Cretan Sea for the first time. The comparison of model response with in situ observations provides a first opportunity for assessment, validation and, more generally, for further model refinement.

The aim of this study is, first, to present the 3D model developed by the coupling of advanced hydrodynamic and ecological models and, secondly, to investigate the interactions between the physical and biogeochemical systems in the Cretan Sea. Emphasis is given in the understanding of the relationship between physical forcing and the evolution of chlorophyll and primary production.

2. Materials and methods

2.1. In situ data

It is only in the last decade that intensive research has taken place in the Cretan Sea through two major research projects: PELAGOS (September 1993–March 1996) (Balopoulos, 1996) and CINCS (May 1994–June 1996) (Tselepides and Polychronaki, 1996), and it is this work which provides the information on the ecosystem function of the region. During the PELAGOS project, only four stations were sampled, two of which were located at the Kassos and Antikithira straits and another two at the outer part of the Cretan sea, in contrast with the CINCS project, where a denser grid of stations was frequently

sampled although the covered area was extended only at the central Cretan shelf and slope. The frequency of sampling during CINCS was bimonthly at standard depths (1, 20, 50, 75, 100, 120, 150, 200, 300, 400, 500, 700, 1000, 1200, 1500 m). The measured parameters were physiochemical (water, temperature, salinity, dissolved oxygen, nutrients, chlorophyll *a* and particulate organic carbon) and biological parameters (primary and bacterial production, pelagic bacteria, phytoplankton and zooplankton). Details of the data collection and analysis can be found in Tselepides and Polychronaki (1996).

Because of the scarcity of the data and the uneven method of result presentation (Gotsis-Skretas et al., 1999; Ignatiades, 1998; Kucuksezgin et al., 1995; Tselepides et al., 2000), the in situ data acquired during CINCS project has been analysed in order to validate the simulation model results. The wider area of Cretan Sea is separated into three subareas: (a) a coastal area, influenced by land activities, thus, exhibiting more mesotrophic characteristics; (b) a transient area with oligotrophic characteristics and (c) an offshore deep area largely influenced by the large-scale hydrodynamics and the presence of the gyral systems. In Fig. 2a, the positions of stations D2, D5 and D7 representative for the above-mentioned areas are shown. Although the main variability is expected along the North–South, the in situ data along the East–West has also been examined in six stations located along transect A (Fig. 2a). This transect parallel to Cretan coastline was chosen in order to provide information on the action and the subsequent effects of the gyral structures.

2.2. Model description

The 3D ecosystem model consists of two, highly portable, on-line coupled submodels: the 3D Princeton Ocean Model (POM) (Blumberg and Mellor, 1987), which describes the hydrodynamics of the area providing the background physical information to the ecological model, and the 1D Cretan sea ecosystem model (Triantafyllou et al., 2002b) based on the European Regional Seas Ecosystem Model (ERSEM) (Baretta et al., 1995) describing the biogeochemical cycles.

POM is a primitive equation, time-dependent, σ-coordinate, free surface, split-mode time step model. It calculates the following equations for the velocity $U_i=(U, V, W)$, temperature T and salinity S.

$$\frac{\vartheta U_i}{\partial x_i} = 0 \tag{1}$$

$$\frac{\vartheta (U,V)}{\vartheta t} + U_i \frac{\partial}{\partial x_i}(U,V) + f(-U,V) = \left(-\frac{1}{\rho_0}\right)\left[\frac{\partial p}{\partial x}, \frac{\partial p}{\partial y}\right] + \frac{\partial}{\partial z}\left[K_{\mathrm{M}} \frac{\partial}{\partial z}(U,V)\right] + (F_U, F_V) \tag{2}$$

$$\frac{\vartheta T}{\vartheta t} + U_i \frac{\vartheta T}{\vartheta x_i} = \frac{\partial}{\partial z}\left[K_{\mathrm{H}} \frac{\partial T}{\partial z}\right] + F_T \tag{3}$$

$$\frac{\vartheta S}{\vartheta t} + U_i \frac{\vartheta S}{\vartheta x_i} = \frac{\partial}{\partial z}\left[K_{\mathrm{H}} \frac{\partial S}{\partial z}\right] + F_S \tag{4}$$

It contains an embedded second-moment turbulence closure submodel (Mellor and Yamada, 1982), which gives the vertical eddy diffusivity parameters K_{M} and K_{H}. The analogous horizontal parameters F_U, F_V, F_T and F_S are calculated through the Smagorinsky (1963) formulation. The density $\rho=\rho(T, S, P)$ is calculated from the UNESCO equation of state adapted by Mellor (1991).

ERSEM uses a 'functional' group approach to describe the ecosystem where the biota is grouped together according to their trophic level (subdivided according to size classes or feeding methods). State variables have been chosen in order to keep the model relatively simple without omitting any component that may exert a significant influence upon the energy balance of the system. The ecosystem is considered to be a series of interacting complex physical, chemical and biological processes, which together exhibit coherent system behaviour. Biological functional growth dynamics are described by both physiological (ingestion, respiration, excretion, egestion, etc.) and population processes (growth, migration and mortality). The biological variables in the model are: phytoplankton, functional groups related to the microbial loop and zooplankton (Baretta-Bekker et al., 1995;

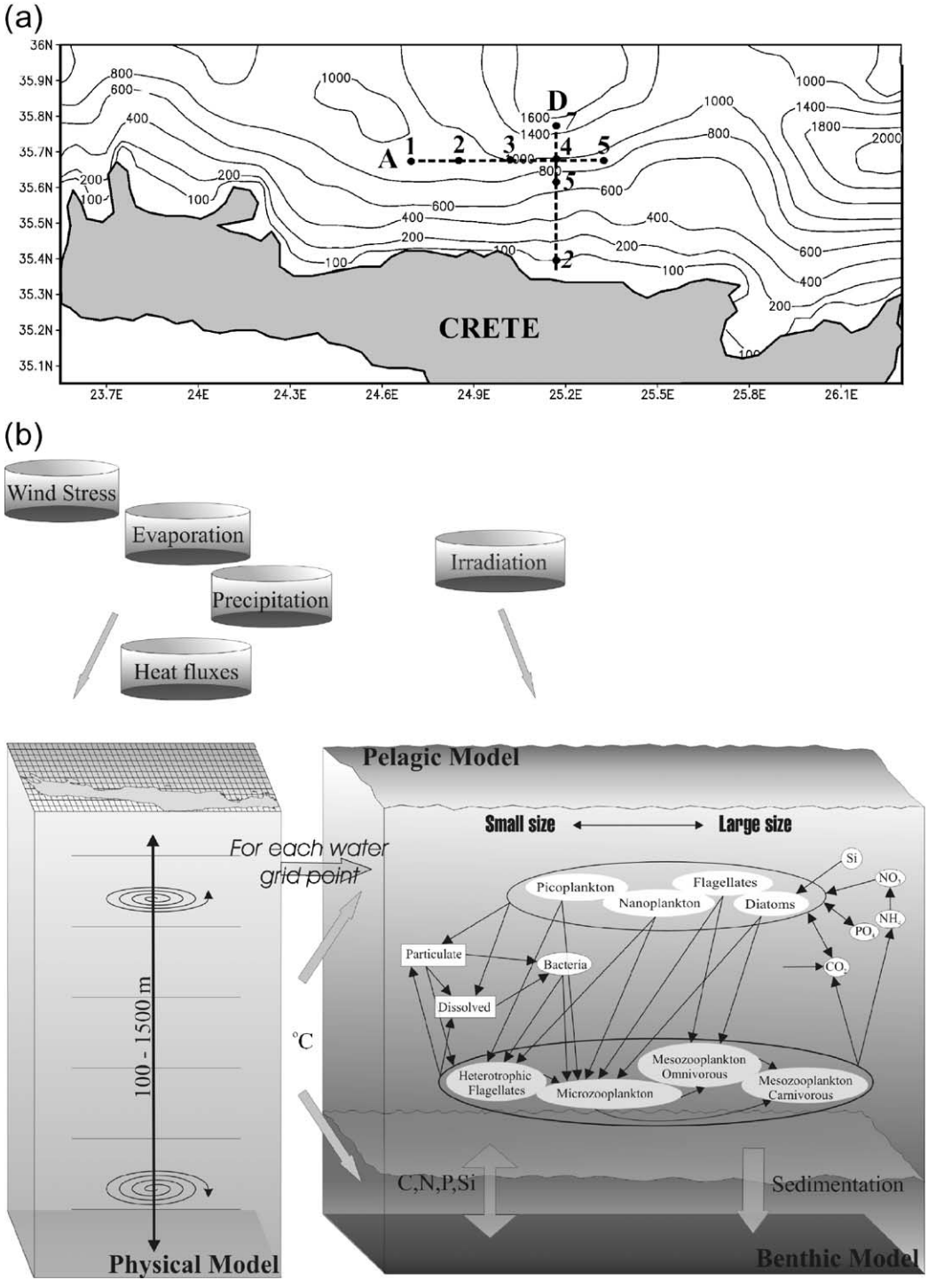

Fig. 2. (a) Simulation domain with in situ data transects, (b) foodweb.

Blackford and Radford, 1995; Broekhuizen et al., 1995; Ebenhoh et al., 1995; Varela et al., 1995). Biologically driven carbon dynamics are coupled to the chemical dynamics of nitrogen, phosphate, silicate and oxygen.

From data analysis and literature (Azov, 1991; Stergiou et al., 1997; Tselepides and Polychronaki, 1996), the model food web has been modified (Fig. 2b) to represent the real system. P4 (dinoflagellates) were made available for grazing by Z5 (microzooplankton) and Z4 (mesozooplankton). To differentiate them from the other phytoplankton groups, P4 were associated with new production (preference for NO_3), while P3 (picoplankton) were associated with regenerated production (preference for NH_4) (Valiela, 1984).

Also, the revised version of bacterial submodel has been used (Triantafyllou et al., 2002a). Pelagic bacteria are assumed to be free-living heterotrophs utilizing particulate and dissolved organic material, produced by the excretion, lysis and mortality of primary and secondary producers as food. The original ERSEM bacterial submodel treated dissolved organic carbon as labile and assumed that its turnover time was so short that it did not accumulate in an appreciable amount. Therefore, it was not represented as a state variable, but made instantaneously available to bacteria (Baretta-Bekker et al., 1995). This is clearly not the case in the Mediterranean Sea (Thingstad and Rassoulzadegan, 1995). Bacterial growth is controlled by the availability of DOC, by the availability of dissolved organic and inorganic nutrients, which allow them to assimilate DOC, and by protozoan grazing (Thingstad and Lignell, 1997).

The phytoplankton pool is described by four functional groups based on size and ecological properties. These are diatoms P1 (silicate consumers, 20–200 μ), nanophytoplankton P2 (2–20 μ), picophytoplankton P3 (<2 μ) and dinoflagellates P4 (>20 μ). All phytoplankton groups contain internal nutrient pools and have dynamically varying C/N/P ratios. The nutrient uptake is controlled by the difference between the internal nutrient pool and external nutrient concentration. The microbial loop contains bacteria B1, heterotrophic flagellates Z6 and microzooplankton Z5, each with dynamically varying C/N/P ratios. Bacteria act to decompose detritus and can compete for nutrients with phytoplankton. Heterotrophic flagellates feed on bacteria and picophytoplankton and are grazed by microzooplankton. Microzooplankton also consume diatoms and nanophytoplankton and are grazed by mesozooplankton. The parameter set used in this simulation is the same as the 1D Cretan Ecosystem Model (Triantafyllou et al., 2002b) and is given in Tables 1 and 2.

In the 3D code, the following equation is solved for the concentration of C for each functional group of the pelagic system:

$$\frac{\vartheta C}{\vartheta t} = -U\frac{\partial C}{\partial x} - V\frac{\partial C}{\partial y} - W\frac{\partial C}{\partial z} + \frac{\partial}{\partial x}\left(A_H\frac{\partial C}{\partial x}\right) + \frac{\partial}{\partial y}\left(A_H\frac{\partial C}{\partial y}\right) + \frac{\partial}{\partial z}\left(K_H\frac{\partial C}{\partial z}\right) + \sum BF \quad (5)$$

where U, V, W represent the velocity field, A_H the horizontal viscosity coefficient and K_H the vertical eddy mixing coefficient, provided by the POM. ΣBF stands for the total biochemical flux, calculated by ERSEM, for each pelagic group.

Eq. (5) is approximated by a finite-difference scheme analogous to that of Eqs. (3) and (4) and is solved in two time steps (Mellor, 1991): an explicit conservative scheme (Lin et al., 1996) for the advection and an implicit one for the vertical diffusion (Richtmyer and Morton, 1994).

The benthic–pelagic coupling is described by a simple first order benthic returns module, which includes the settling of organic detritus into the benthos and diffusional nutrient fluxes into and out of the sediment.

2.3. Model set-up

The computational domain covers the Cretan Sea between 23.55° and 26.3°E and 35.05° and 36.0°N, with 56 × 20 grid points, and constant grid spacing in latitude and longitude of 1/20 × 1/20°. The vertical structure is resolved by 30 sigma levels with logarithmic distribution near the surface so as to correctly simulate the dynamics of the surface mixed layer. The bottom topography has been based on the US Naval Oceanographic Office (NAVOCEANO) Data Warehouse (DBDBV), enriched with measurements for the

Table 1
Parameters of the phytoplankton functional groups

Parameter	Name	P1	P2	P3	P4
Environmental effects					
Characteristic Q10	q10ST$	2.0	2.0	2.0	2.0
Uptake					
Maximum specific uptake at 10 °C	sumST$	***1.0***	***1.2***	***1.3***	***1.0***
Loss rates					
Excreted fraction of uptake	pu_eaST$	0.05	0.2	0.2	0.05
Nutrient-lysis rate	sdoST$	0.05	0.05	0.05	0.05
Nutrient-lysis rate under Si limitation	sdoST$	0.1	–	–	–
Respiration					
Rest respiration at 10 °C	srsST$	0.15	0.1	0.1	0.1
Activity respiration	pu_raST$		0.25	0.25	0.25
Nutrient dynamics					
Min N/C ratio (mol g C^{-1})	qn1ST$	0.00687	0.00687	0.00687	0.00687
Min P/C ratio	qp1ST$	0.4288E − 3	0.4288E − 3	0.4288E − 3	0.4288E − 3
Redfield N/C ratio	qnRST$	0.0126	0.0126	0.0126	0.0126
Redfield P/C ratio	qpRST$	0.7862E − 3	0.7862E − 3	0.7862E − 3	0.7862E − 3
Multiplic fact min N/C ratio	xqcSTn$	1.0	1.0	1.0	1.0
Multiplic fact min P/C ratio	xqcSTp$	1.0	1.0	1.0	1.0
Multiplic fact max N/C ratio	xqnST$	***2***	***2***	***2***	***2***
Multiplic fact max P/C ratio	xqpST$	***2***	***2***	***2***	***2***
Maximum Si/C ratio	qsSTc$	0.03	–	–	–
Affinity for NO_3	quSTn3$	0.0025	0.0025	0.0025	0.0025
Affinity for NH_4	quSTn4$	0.0025	0.0025	0.0025	0.0025
Affinity for P	quStp$	0.0025	0.0025	0.0025	0.0025
Half-value of Si limitation	chSTs$	0.3	–	–	–
Sedimentation					
Nutrient limitation value for sedimentation	esNIST$	0.7	0.75	0.75	0.75
Sinking rate (m day^{-1})	resSTm$	5.0	0.0	0.00	0.00

P1 = diatoms, P2 = nanoalgae, P3 = picoalgae, P4 = dinoflagellates. The parameters that have been changed from the standard ERSEM version 11 are indicated in bold italics. Parameter names used follow the nomenclature described in Blackford and Radford (1995).

coastal zone collected by the Institute of Marine Biology of Crete (IMBC).

For the initialisation, forcing and boundary conditions, all available Mediterranean Oceanic Data Base (MODB) (Brasseur et al., 1996) and European Centre for Medium-Range Weather Forecasts (ECMWF) data were objectively analysed to filter out spatial noise and interpolated to grid points where data were missing. The scheme used is an iterative difference-correction scheme (Cressman, 1959) as described by Levitus (1982). The model is initialised with MODB March temperature and salinity fields. The initial conditions for the biogeochemical parameters are taken from the January 1D ecosystem model simulation for station D5 (Triantafyllou et al., 2002b). A uniform field of all state variables is applied to the model domain. The model was run perpetually for 10 years to reach a quasi-steady state and to obtain inner fields fully coherent with the boundary conditions.

Surface boundary conditions of the model include the momentum, heat and salinity fluxes, where the

Table 2
Parameters of microzooplankton functional groups and bacteria

Parameter	Name	B1	Z6	Z5
Environmental effects				
Characteristic Q10	q10ST$	2.95	2.0	2.0
Half oxygen saturation	chrSTo$	0.3125	7.8125	7.8125
Uptake				
Half saturation value	chuSTc$	30.0	250	200
Maximum specific uptake rate 10 °C	sumST$	***0.8***	5.0	1.2
Availability of P1 for ST	suP1_ST$	–	0.0	***1.0***
Availability of P2 for ST	suP2_ST$	–	0.0	***0.4***
Availability of P3 for ST	suP3_ST$	–	***0.4***	0.0
Availability of P4 for ST	suP4_ST$	–	0.0	***1.0***
Availability of Z5 for ST	suZ5_ST$	–	0.0	1.0
Availability of Z6 for ST	suZ6_ST$	–	0.2	1.0
Availability of B1 for ST	suB1_ST$	–	1.0	0.0
Selectivity	minfoodST$	–	100	30
Loss rates				
Assimilation efficiency	puST$	***0.25***	0.4	0.5
Assimilation efficiency at low temperature	puSTo$	0.2	–	–
Excreted fraction of uptake	pu_eaST$	–	0.5	0.5
Excretion				
Fraction of excretion production to DOM	pe_R1ST$	–	0.5	0.5
Mortality				
Oxygen-dependent mortality rate	sdSTo$	–	0.25	0.25
Temperature-independent mortality	sdST$	0.001	0.05	0.05
Respiration				
Rest respiration at 10 °C	srsST$	0.01	0.02	0.02
Nutrient dynamics				
Maximum N/C ratio	qnSTc$	0.0208	0.0167	0.0167
Maximum P/C ratio	qnSTc$	0.00208	0.00167	0.00167

Z5 = microzooplankton, Z6 = heterotrophic flagellates and B1 = bacteria. The parameters that have been changed from the standard ERSEM version 11 are indicated in bold italics. Parameter names follow the nomenclature described in Blackford and Radford (1995).

ECMWF (1979–1993) 6-h interval wind stresses and the monthly heat flux data were used. For the heat budget at the surface, a further correction coefficient C_1 is set to 10 W/m^2/°C to adjust heat flux to the Cretan Sea modelling area:

$$\rho C_p K_H \frac{\partial T}{\partial z}\Big|_{z=0} = Q_T + C_1(T^* - T) \quad (6)$$

where ρ is the air density, C_p the specific heat capacity, Q_T the total heat flux field and T^* the MODB sea surface temperature.

The salinity boundary condition at the surface is given by:

$$K_H \frac{\partial S}{\partial z}\Big|_{z=0} = S(E - P) + C_2(S^* - S) \quad (7)$$

where S^* is the MODB sea surface salinity, P is the Jaeger (1976) monthly precipitation rate and E is the evaporation rate calculated from the latent heat flux. The correction term $C_2(S^*-S)$ is used as a further adjustment for the imperfect knowledge of $E-P$. The coefficient C_2 is set to 0.7 m/day, based on sensitivity studies. Incident sea surface radiation was calculated from the latitude and modified by the cloud cover data using the methods of Patsch (1994).

Along the west, north and east boundaries, the following open boundary conditions have been used.

Upstream advection equation for the temperature (T) and salinity (S):

$$\frac{\vartheta T}{\vartheta t} + U\frac{\partial T}{\partial x} = 0 \tag{8}$$

and where an inflow, T and S are specified by the MODB monthly climatology. These data sets initially have been smoothed by a first-order Shapiro filter to eliminate small-scale noise.

The normal barotropic velocities are described by the Sommerfeld radiation condition:

$$\overline{U} = \varepsilon\sqrt{\frac{g}{\mathrm{H}}}\zeta + \overline{U}_{\mathrm{ext}} \tag{9}$$

where ε depends on the position of the open boundary, and is equal to $+1$ for the eastern and northern boundary and -1 for the western boundary.

While the free-wave radiation condition is used for the vertically integrated velocity perpendicular to the boundary, the baroclinic velocity on the open boundaries is the same as the interior grid point closest to the boundary.

The ecosystem pelagic state variables are described by solving water column 1D ecosystem models at each grid point along the open boundaries.

2.4. Validation

The presentation and validation with scarce in situ data of 3D ecosystem model results is a difficult task. To resolve this problem a cost function is used as a validation method (Moll, 2000). This cost function is a mathematical function, which enables us to compare model results with in situ data, and its outcome is a nondimensional value, which is indicative of how close, or how distant two particular values are. The function used is:

$$C_{x,t} = \frac{M_{x,t} - D_{x,t}}{sd_{x,t}} \tag{10}$$

where $C_{x,t}$ is the normalised deviation between model and data for box x and season t, $M_{x,t}$ the mean value of the model results within box x and season t, $D_{x,t}$ the mean value of the in situ data within box x and season t and $sd_{x,t}$ the standard deviation of the in situ data within box x and season t.

The cost function results give an indication of the goodness of fit of the model by providing a quantitative measure of deviation, normalised in units of standard deviation of data. The lower the absolute value of the cost function, the better the agreement between model and data. In this work, the same categories of cost function results described by Moll (2000) (<1 = very good, 1–2 = good, 2–5 = reasonable, >5 = poor) were used.

3. Results and discussion

3.1. Hydrodynamics

The hydrodynamic model was spun up for 10 years to reach a quasi-steady state, and the results of the 11th year are presented as 10-day averages. The model reproduces similar circulation characteristics in the area as revealed by the analysis and synthesis of the PELAGOS data set (Fig. 3). Fig. 4a and b shows the circulation of the Cretan Sea at 50 m, which is characterized by a succession of cyclonic and anticyclonic eddies interconnected by meandering currents around their peripheries. The dominant eddies that play a significant role in the circulation of the upper layers are the central anticyclone and the eastern cyclone. The central anticyclone exhibits spatial and temporal variability in terms of its intensity while the eastern cyclone is prominent both during winter and summer. The complex structure of the area is completed by smaller eddies intensified or weakened by depth.

At intermediate depths (200 m), during February, a succession of smaller cyclonic and anticyclonic features interconnected by a meandering current, with

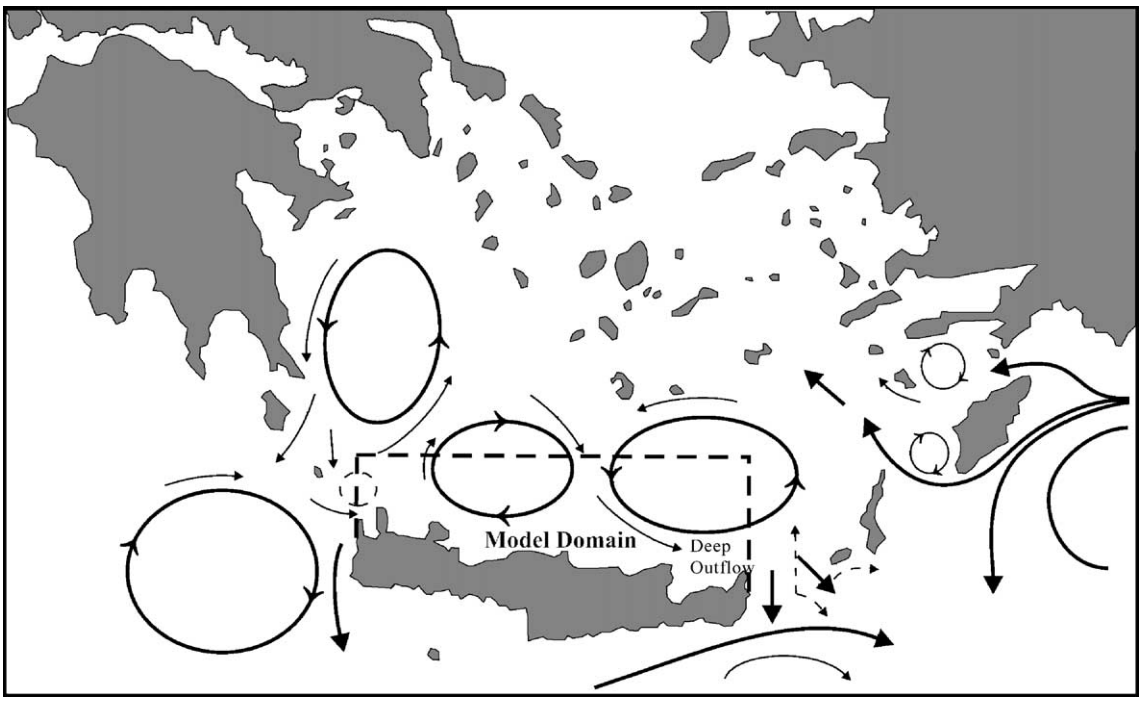

Fig. 3. Schematic configuration of the main upper thermocline circulation modified after Theocharis et al. (1999).

intense appearance of the central anticyclone is simulated. During August, at the same depths, the east–west currents are intensified and the cyclonic circulation remains prominent, while the anticyclone has been elongated into an east–west direction (Fig. 4c and d).

A model improvement would be the application of detailed information on the open boundaries, which in this study were not available.

3.2. Ecosystem validation

After reaching steady state, the mean values of modelled nutrients (phosphate, nitrate, ammonia and silicate) and chlorophyll were taken along the two transects for the four seasons and the cost function was calculated. Results are given in Fig. 5. For the offshore stations (depth >150 m), the water column is separated into two layers, the upper (0–150 m) describing the euphotic zone with major biological activity and the lower (150–bottom) where conditions are more stable with reduced biological activity and, hence, small variability of nutrients.

At the coastal station (D2) along transect D, the results are very good, with the only exceptions being phosphate during summer and winter and chlorophyll in winter. At station D5, the simulations of the upper layer for nutrients and chlorophyll vary from very good to good. Only phosphate in summer and ammonia in winter fall within the scale of reasonable values. For the deeper layer, although chlorophyll and nitrate simulations remain very good, the silicate results are reasonable which is also the case for ammonia during winter and summer. Simulated phosphate shows a good fit during winter and spring, and a reasonable fit for the remaining two seasons. An explanation for the deterioration of model results in the deeper layers is attributed to the presence of the aperiodic water masses (TMW, LIW) penetrating the area and affecting the concentrations of nutrients. At the outer station (D7), the simulation of the euphotic zone is very good for most parameters, with the exception of ammonia and silicate where it is considered good and in one occasion reasonable (silicate during winter). In the deeper layer, the results are similar to those of station D5, reinforcing the aspect that sporadic water masses

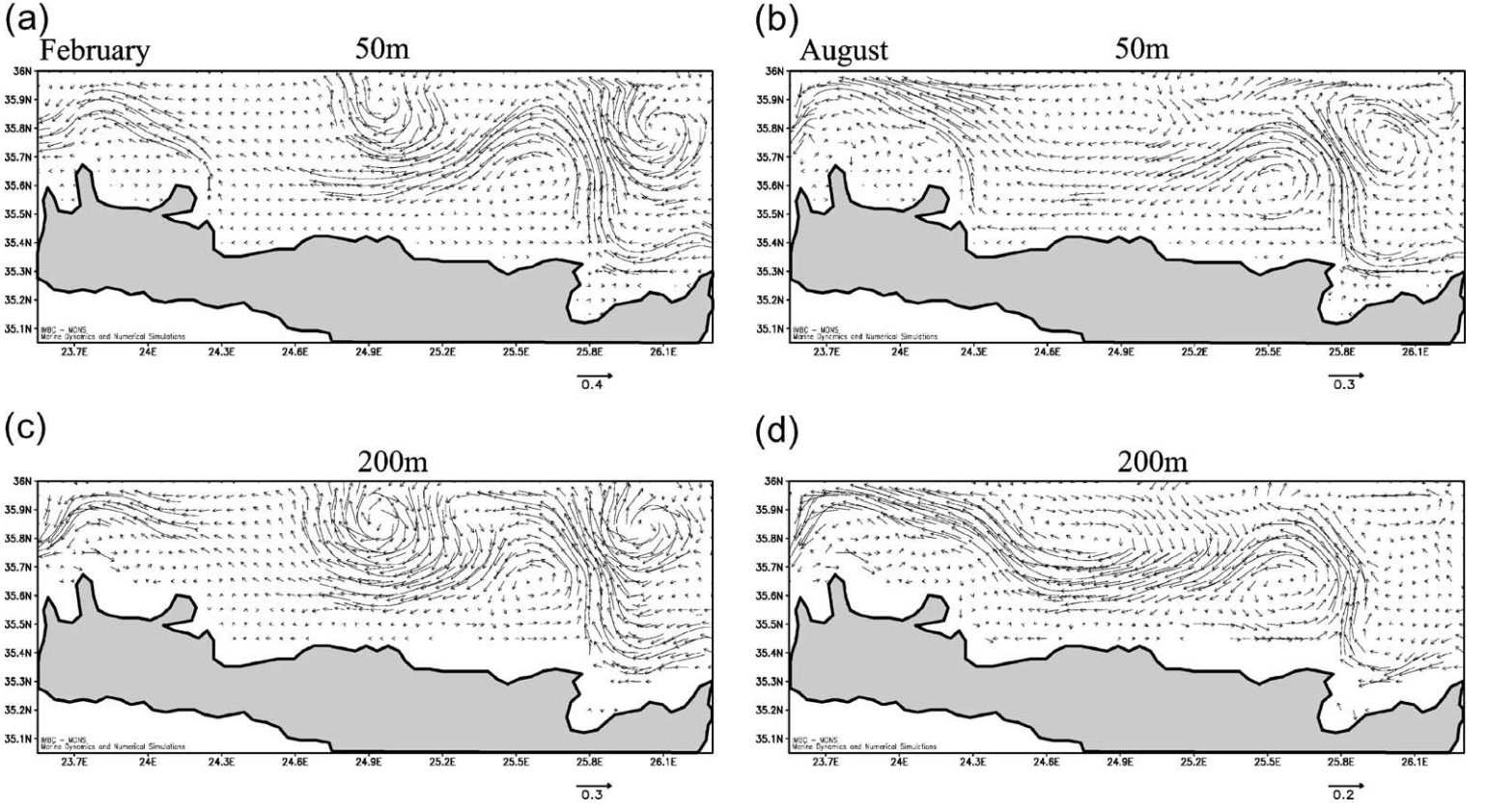

Fig. 4. Model velocity fields at (a) 50 m during February, (b) 50 m during August, (c) 200 m during February and (d) 200 m during August.

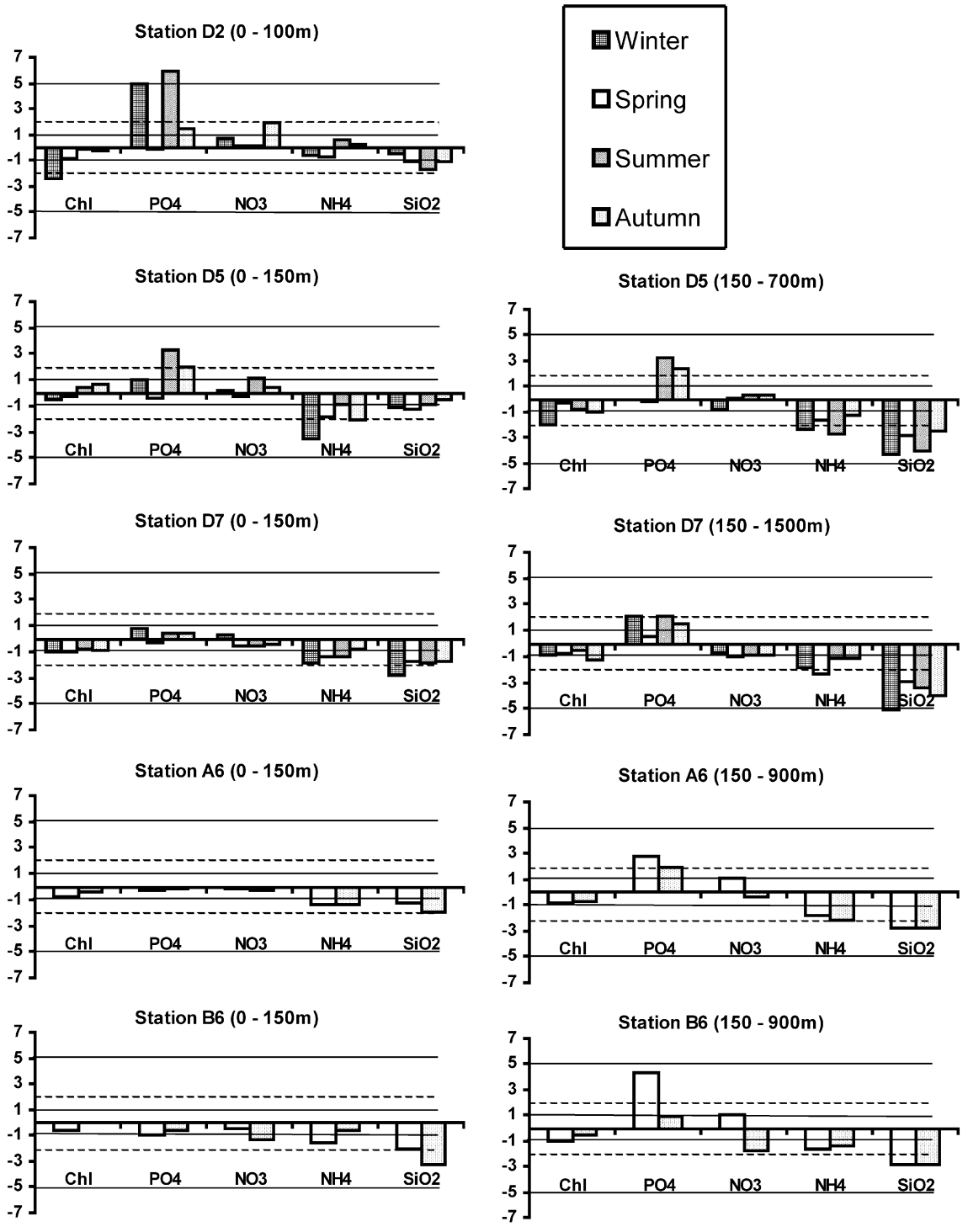

Fig. 5. Nitrate, phosphate, ammonia, silicate and chlorophyll validation results along transect D for the upper and lower water column. The cost function is in units of standard deviation for the four seasons.

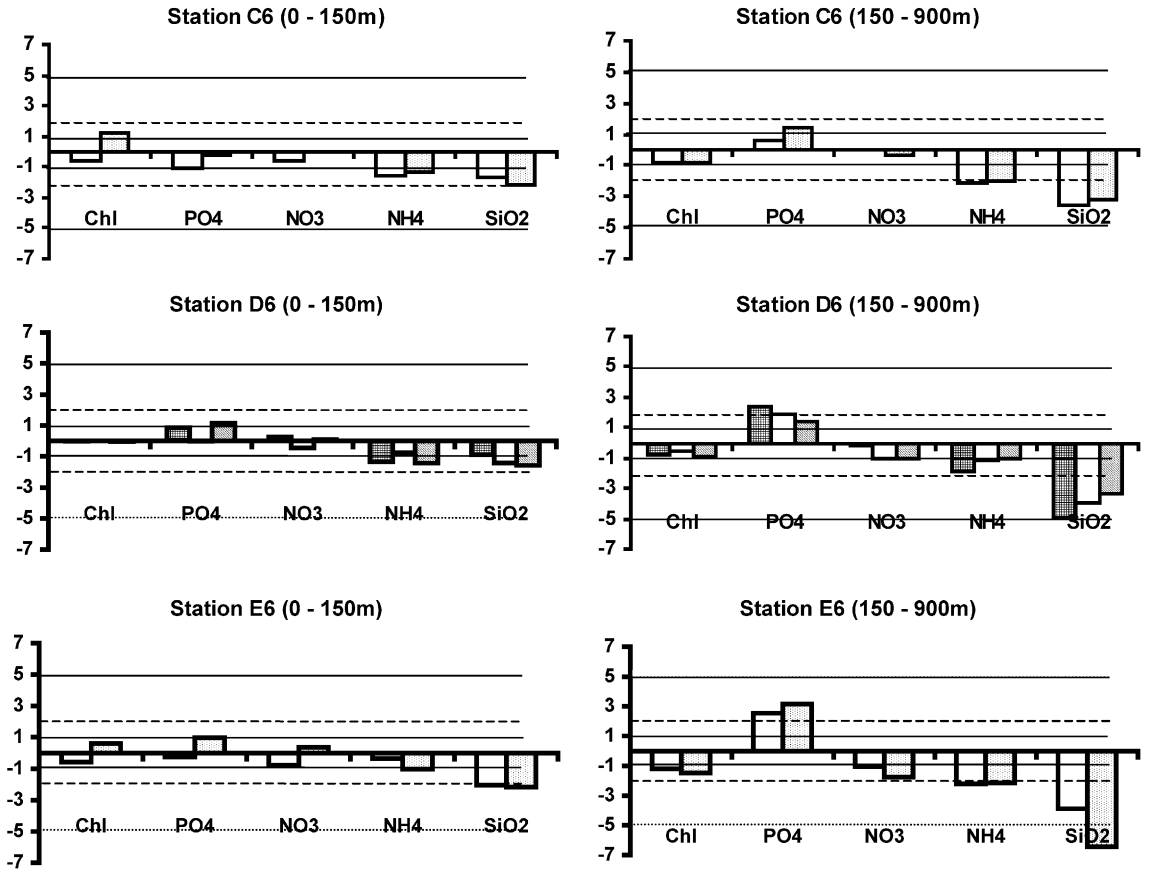

Fig. 5 (*continued*).

affect the concentrations of nutrients leaving unaffected the concentration of chlorophyll. The signal of this water mass has been reported during the CINCS project at the outer stations (D5 and D7) (Tselepides et al., 2000), and is characterised by an intrusion of water with higher concentrations of nitrate and lower salinities at 400–450 m (Fig. 6). The vertical distribution of chlorophyll as produced by the model (Fig. 7), indicates a deep chlorophyll maximum (DCM) at 60 m in contrast with the in situ data where the DCM is located between 80 and 90 m (Fig. 8). This may be attributed to the fact that the model is using a fixed carbon/chlorophyll ratio, thus, expressing the depth of maximum biomass. Tselepides et al. (2000) found that the DCM in the Cretan Sea was coincident with the minima in phytoplankton cell densities suggesting that the cells in the deeper layer contained higher chlorophyll content. At the outer stations (D5, D7), in situ chlorophyll levels exhibit a characteristic DCM with concentrations ranging from 0.03 to 0.24 μg l^{-1} at around 90 m for an extended period (7/94–5/95), while the chlorophyll signature is found down to 250 m indicating strong vertical processes (Tselepides et al., 2000).

Looking at the East–West transect, although the in situ data is concentrated to mainly two seasons (Spring and Autumn), interesting conclusions can be drawn regarding the behaviour of the model. As with the deeper stations on transect D, the water column is separated into two layers. At the western station A1, the simulation of chlorophyll, phosphate and nitrate in the top layer are characterised as very good and those of ammonia and silicate as good. In the deeper layer at the same station, the model results

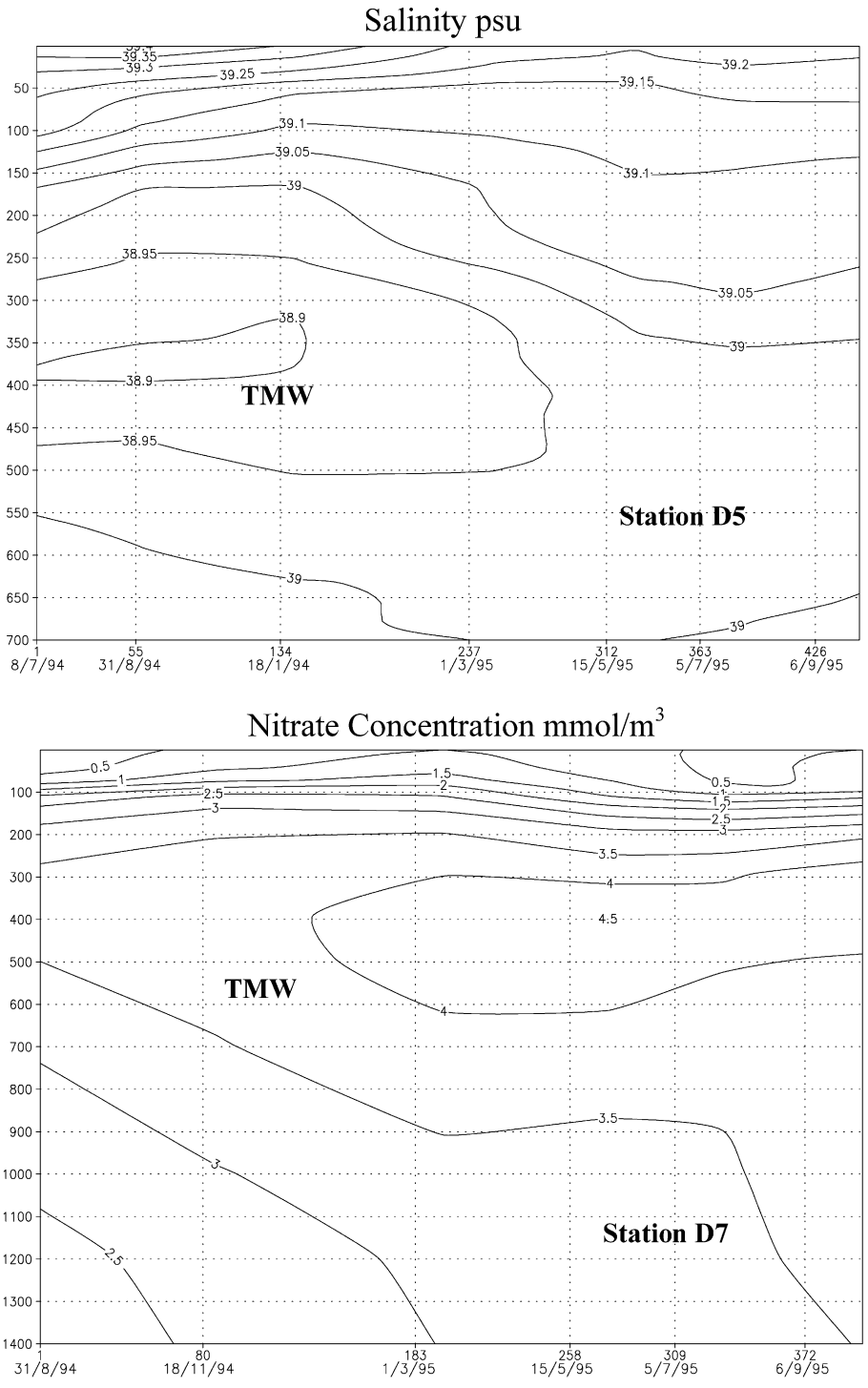

Fig. 6. Transient Mediterranean water signal in in situ data at stations D5 and D7.

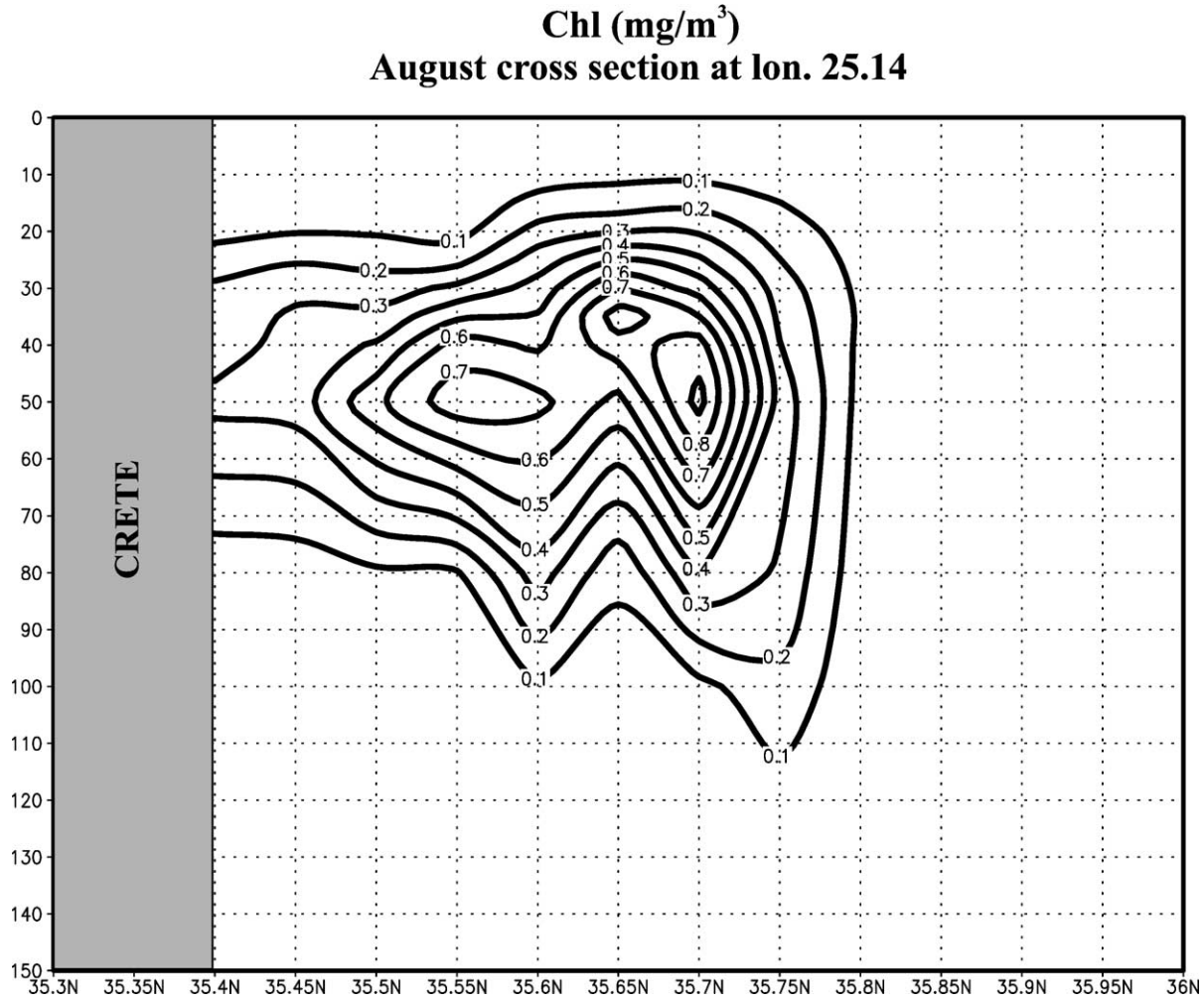

Fig. 7. Modelled vertical distribution of chlorophyll concentrations.

are less satisfactory. Moving towards east at the surface layer of station A2, with the exception of silicate, there are good or very good model results. Again, the model is less satisfactory at the lower layer. For the rest of the stations (A3, A4, A5), the picture is mainly the same with the upper part of the water column being simulated more efficiently than the deeper with silicate being the variable simulated least successfully followed by ammonia. A further characteristic is the lack of significant differentiation between seasons.

The cost function scores for both transects expressed as percentages are indicative of the model's overall performance. Thus, for the upper layer, 60% of the results are very good, 30% good, 10% reasonable and only one score was in the poor category (0.1%). In the deeper layer, 34% of the results were very good, 28% good, 36% reasonable and 2% poor. It is obvious that the model is behaving better at the surface layer, which is more biologically significant and less efficiently at the deeper zone. This can be attributed partly to the fact that midwater biogeochemical processes are not explicitly represented in ERSEM and partly to the presence of water masses with distinct characteristics as mentioned before. The behaviour of the model does not differentiate significantly along the two transects producing similar scores for the upper and lower parts of the water column.

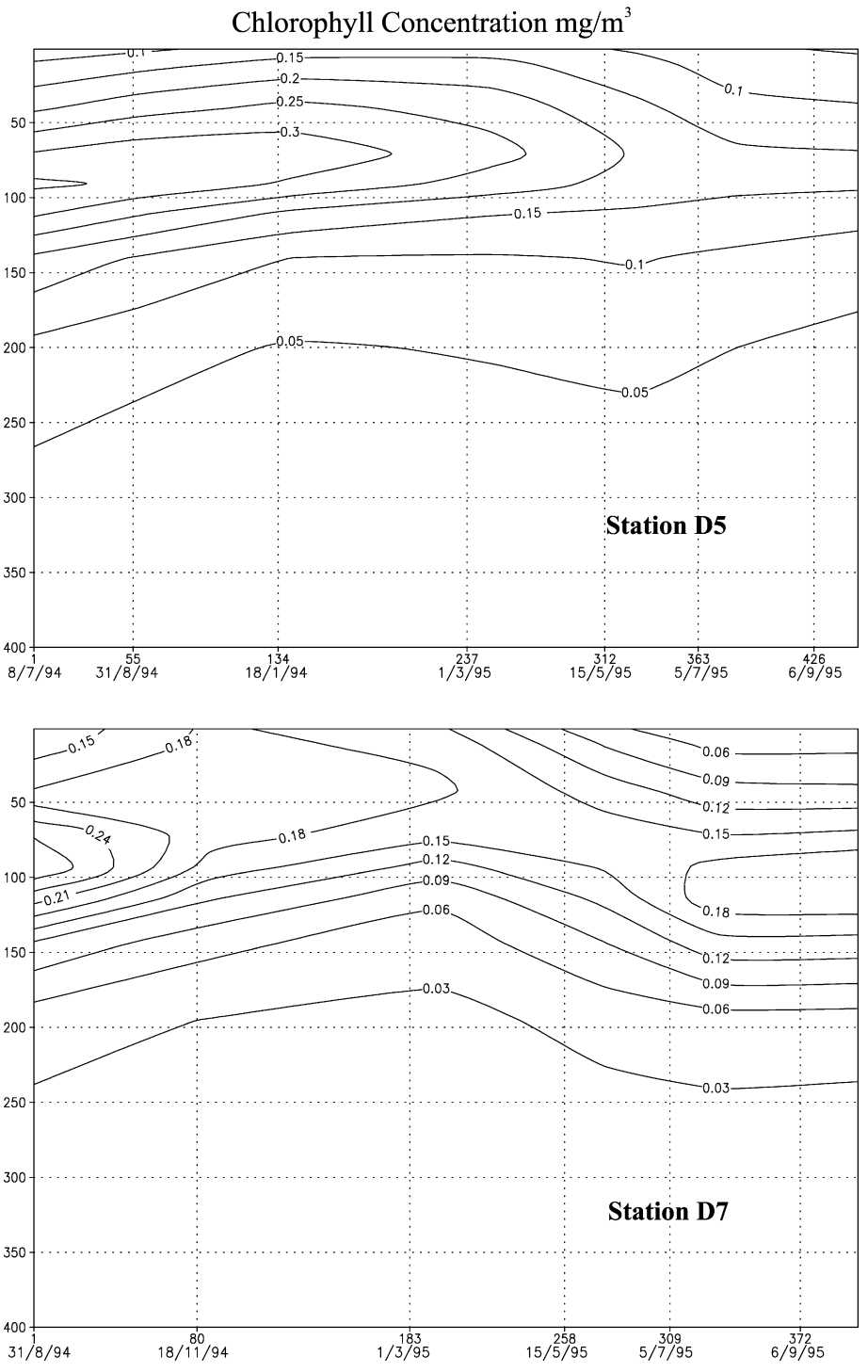

Fig. 8. Observed deep chlorophyll maximum at stations D5 and D7.

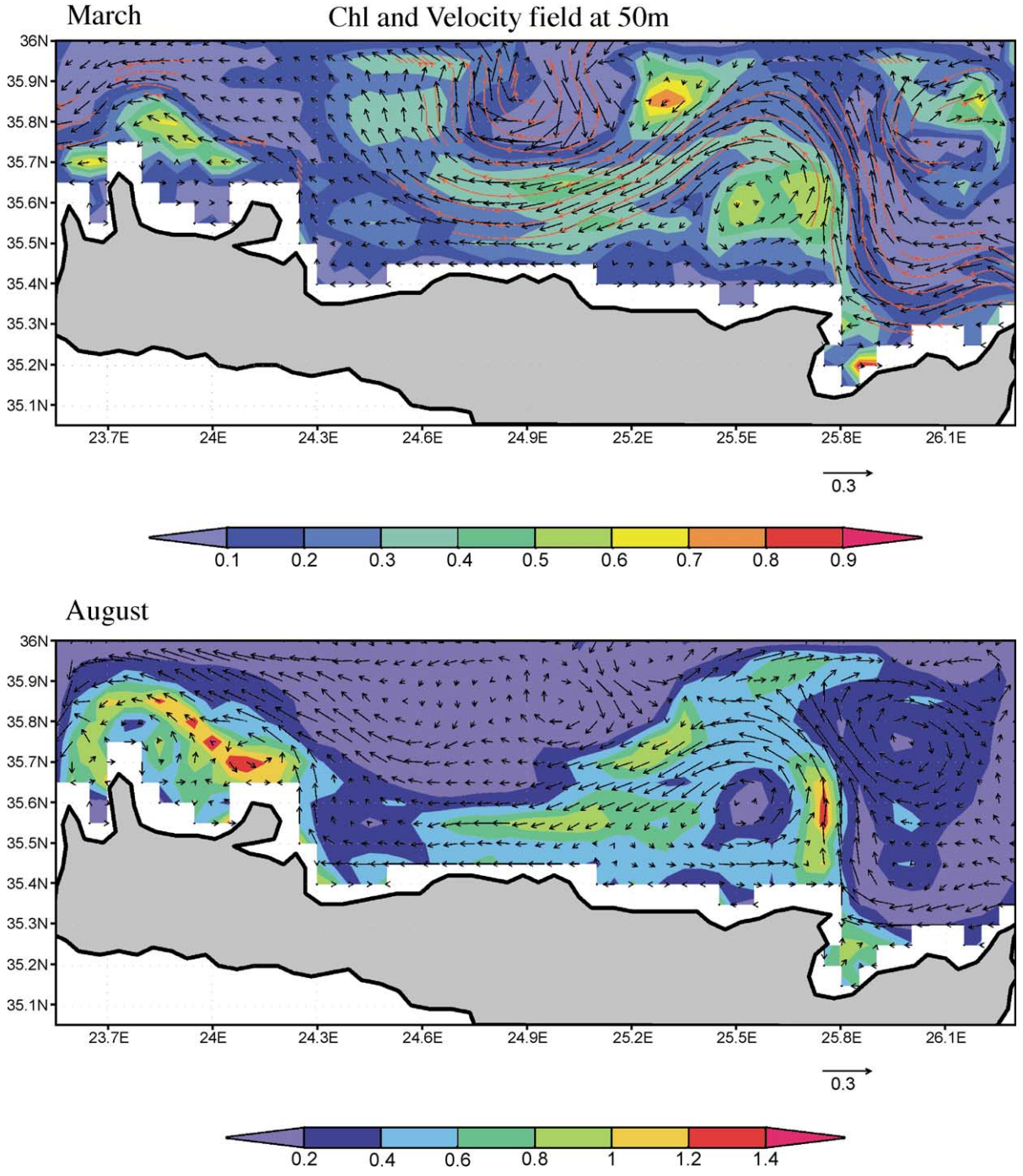

Fig. 9. Velocity field and chlorophyll concentrations for March and August at 50 m.

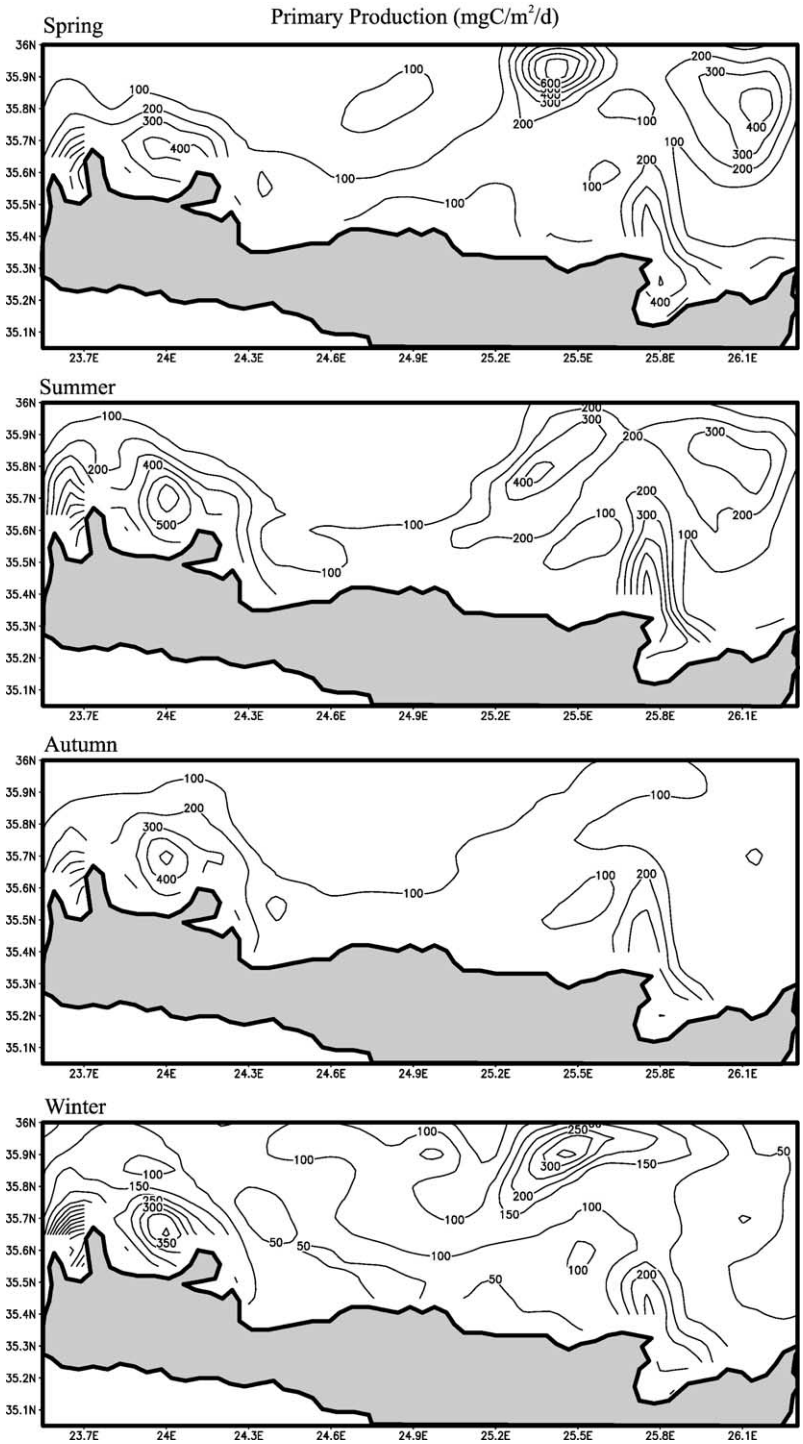

Fig. 10. Primary production for the four seasons integrated to 100-m depth.

The biology in the Cretan sea is largely governed by the hydrological patterns and in particular by the gyral dipole, with chlorophyll concentrations closely following the circulation patterns (Fig. 9). The cyclonic circulation to the north of the central and eastern part of the island is prominent both in March and August, while the anticyclonic circulation at the north central part decreases significantly in the sum-

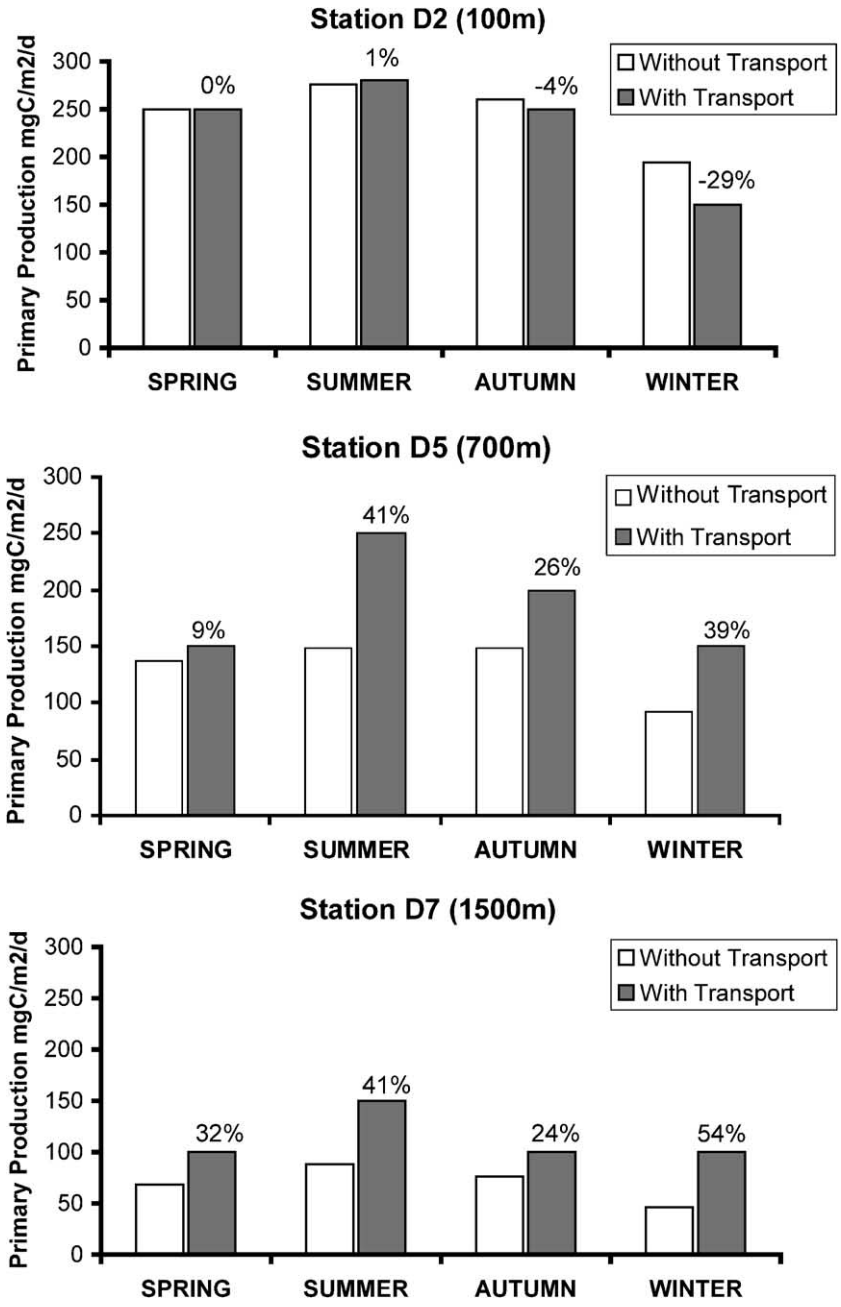

Fig. 11. Primary production at stations D2, D5 and D7 with and without transport. Values on top of the bars represent the difference in production due to transport.

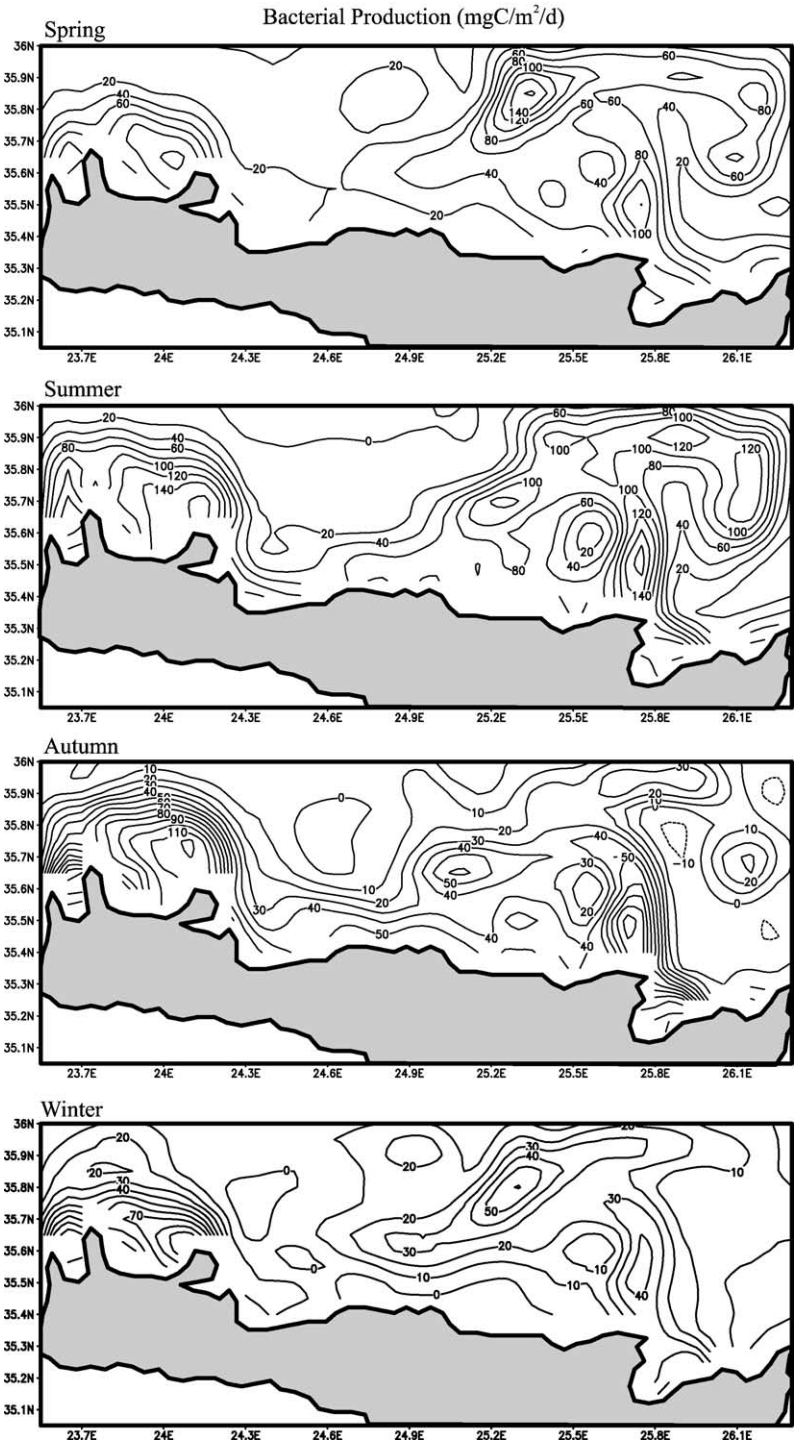

Fig. 12. Bacterial production for the four seasons integrated to 100-m depth.

mer. This pattern results in areas of increased production around the cyclone and very low production at the centre of the anticyclone.

3.3. Primary and bacterial production

The spatial variability of the mean primary production for the four seasons integrated over the top 150 m is investigated (Fig. 10). The Cretan Sea is oligotrophic with low annual productivity (30–80 g C m^{-2} $year^{-1}$) and maximum rates between late winter and early spring (Psarra et al., 2000). During this period, highest model values of primary productivity are found between the two main gyral systems while lower concentrations are as expected at the centre of the anticyclone. The model results are in accordance with the field observations where increase in the intensity of the eddy dipole in the Cretan Sea has been observed during that period (Souvermezoglou et al., 1999). Primary and bacterial production decrease moving offshore while the increased production rates during winter and spring are due to intense mixing

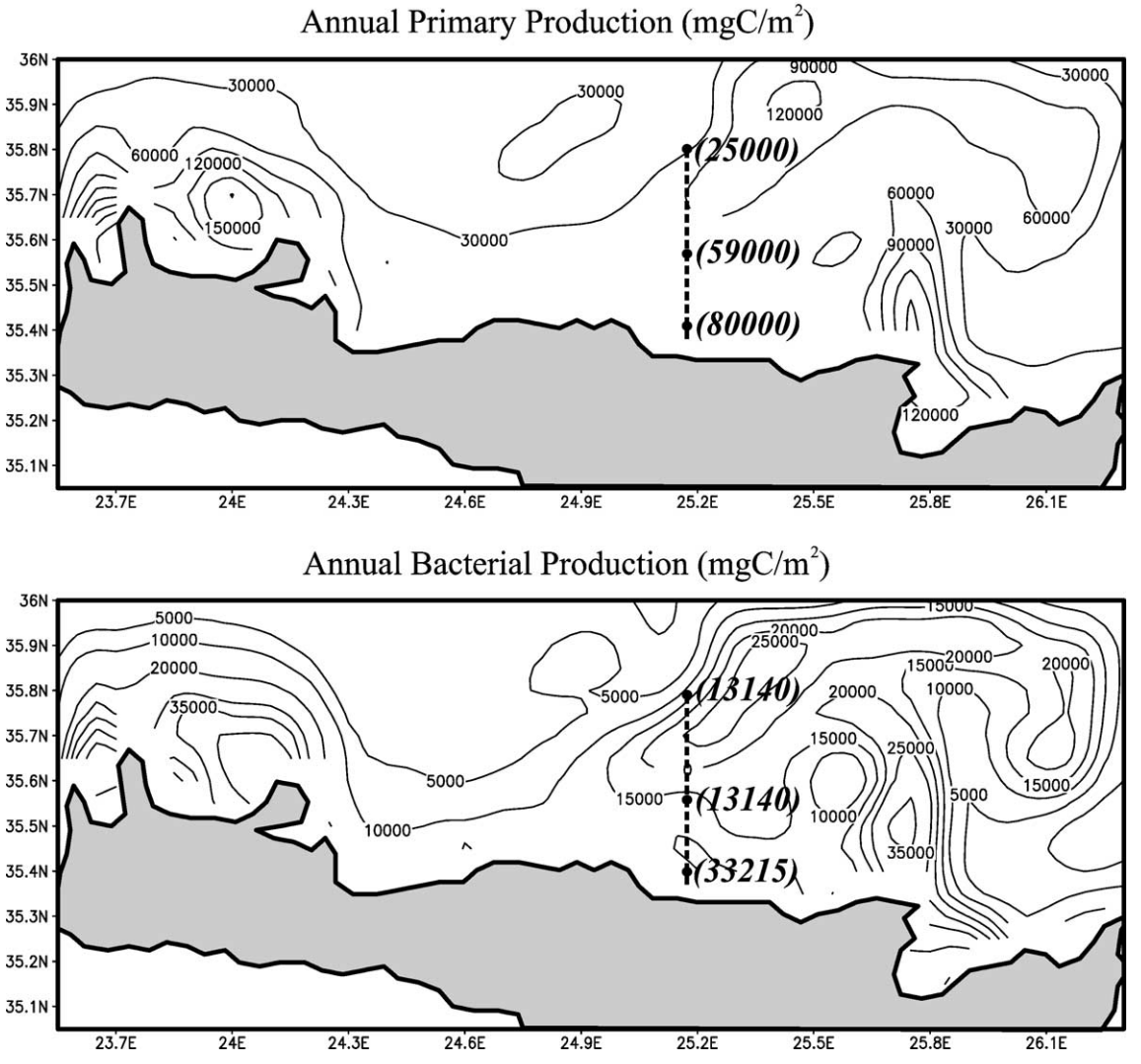

Fig. 13. Model annual primary and bacterial production integrated to 100-m depth. Observational data along the transect are given in brackets (Ignatiades, 1998; Psarra et al., 2000; Van Wambeke et al., 2000).

and subsequent supply of nutrients to the photic zone, triggering production (new production). An interesting feature is the formation of high production areas away from the coast in the central-east part of the model domain. To explore the underlying dynamics, two model runs were performed with and without transport along the D transect. Fig. 11 shows that close to the coast (station D2), the absence of transport does not cause significant differences in the primary production. However, this is not the case during winter when the transport causes a 29% reduction in primary production. This is explained by the fact that in winter the strong North winds cause the downwelling of water transferring nutrients to the deep layers increasing, thus, the oligotrophy of the area close to the coast. Moving to deeper stations, the application of transport results in the increase of primary production due to the injection of waters from the deeper layers with maximum effect during summer. The above demonstrate that the ecology of the offshore system is highly dependent in the hydrodynamic features present, especially during summer when due to the nutrient limitation conditions, small injections of nutrients have significant effects in the primary production (41%). Increased rates are retained during summer due to activity below the thermocline (regenerated production).

Mean daily bacterial production (Fig. 12) follows the primary production quite closely exhibiting similar patterns indication of a strong coupling between the two groups. Once again, rates are higher at the west decreasing towards the east while the increased values at latitude 25.8 are due to the presence of the cyclone. The annual integrated values of primary and bacterial production (Fig. 13) compare very well with the values measured along transect D (Psarra et al., 2000; Van Wambeke et al., 2000) as well as in the outer Cretan Sea (Ignatiades, 1998). Overall model values are within the ranges measured indicating three areas of high production, the west part of the island, the eastern part at latitude 25.8° and the north part at 25.4° latitude. High production in these areas is the outcome of the prevailed flow regime where waters are pushed to the west with a distinct cyclone at the eastern part. In the eastern Mediterranean, the observed depth integrated bacterial production is 18–54% (mean 34%) of the integrated primary production (Turley et al., 2000). Considering a bacterial growth efficiency of 20%, then 89–268% (mean 170%) of primary production is required to support the bacterial carbon demand. Thus, bacterial production is entirely dependent on primary production products (Turley et al., 2000). The increasing oligotrophy towards the east is exhibited during all four seasons with the west part having twice as high rates. Another important characteristic is the low productivity close to the central Cretan coast during winter with rates increasing during spring.

4. Conclusions

This paper shows how the development and the application of a 3D biogeochemical model can be used as a tool to provide knowledge on the functioning of the oligotrophic Cretan Sea ecosystem. Modelled nutrients, chlorophyll, bacterial and primary production have been validated and shown to fit with in situ data. A cost function was used for validation and proved to be an important mathematical tool for comparing model results with observational data. The increased scores of the cost function in the deeper layers are attributed to inaccurate initialisation of model parameters due to the presence of distinct water masses with different physicochemical characteristics.

The regional variation of the ecosystem parameters is a consequence of the circulation patterns of the area illustrating the necessity of a 3D complex ecosystem model. Simulations support the hypothesis that the ecosystem dynamics of the Cretan Sea are mainly driven by the hydrodynamics. Throughout this simulation study, a double-gyre system consisting of an anticyclone to the west and a cyclone to the east interconnected by meandering currents is persistent in the region with a significant variability in location, shape and intensity. The influence of this can be seen in the productivity of the Cretan Sea, with higher values between the gyral dipole and lower values at the centre of the anticyclone. Modelled annual primary and bacterial productivity was found to be within the range of data reported in the literature.

The existence of a numerical model that efficiently describes the ecosystem of the Cretan Sea presented in this paper establishes the numerical basis for the development of a forecasting system capable of sup-

porting coastal zone management issues. Such a system will use numerical models in conjunction with observational data and data assimilation techniques.

Acknowledgements

This work was partially supported by the Mediterranean Forecasting System Pilot Project MAS3-PL97-1608. The authors would like to thank Mrs. A. Pollani for her substantial help, Professor A. Eleftheriou for his constructive criticism during the preparation of this work, Mrs. M. Eleftheriou for her help in editing this text and K. Georgiou for software assistance.

References

Allen, J.I., Blackford, J.C., Radford, P.J., 1998. An 1-D vertically resolved modelling study of the ecosystem dynamics of the middle and southern Adriatic Sea. Journal of Marine Systems 18, 265–286.

Azov, Y., 1986. Seasonal patterns of phytoplankton productivity and abundance in nearshore oligotrophic waters of the Levant Basin (Mediterranean). Journal of Plankton Research 8 (1), 41–53.

Azov, Y., 1991. Eastern Mediterranean—a marine desert? EMECS'90 23, 225–232.

Balopoulos, E.T., 1996. PELAGOS. MAS2-CT93-0059, NCMR, Athens.

Balopoulos, T.E., et al., 1999. Major advances in the oceanography of the southern Aegean Sea–Cretan Straits system (eastern Mediterranean). Progress in Oceanography 44, 109–130.

Baretta, J.W., Ebenhoh, W., Ruardij, P., 1995. The European Regional Seas Ecosystem Model, a complex marine ecosystem model. Netherlands Journal of Sea Research 33, 233–246.

Baretta-Bekker, J.G., Baretta, J.W., Rasmussen, E., 1995. The microbial foodweb in the European Regional Seas Ecosystem Model. Netherlands Journal of Sea Research 33, 363–379.

Becacos-Kontos, T., 1977. Primary production and environmental factors in an oligotrophic biome in the Aegean Sea. Marine Biology 42, 93–98.

Bergamasco, A., Carniel, S., Pastres, R., Pecenik, G., 1998. A unified approach to the modelling of the Venice lagoon-Adriatic sea ecosystem. Estuarine Coastal and Shelf Science 46, 483–492.

Berland, B., Bonin, D., Maestrini, S., 1980. Azote ou phosphore? Considerations sur le "paradoxe nutrionnel" de la Mer Mediterranee. Oceanologica Acta 3, 135–142.

Berman, T., Azov, Y., Townsend, D., 1984. Understanding oligotrophic oceans: can the eastern Mediterranean be a useful model. In: Holm-Hansen, O., Bolis, L., Giles, R. (Eds.), Lecture Notes on Coastal and Estuarine Studies. Springer-Verlag, Berlin, pp. 101–112.

Blackford, J., Radford, P., 1995. A structure and methodology for marine ecosystem modelling. Netherlands Journal of Sea Research 33, 247–260.

Blumberg, A.F., Mellor, G.L., 1987. A description of a three-dimensional coastal ocean circulation model. In: Heaps, N.S. (Ed.), Three-Dimensional Coastal Ocean Circulation Models. Coastal Estuarine Science. AGU, Washington, DC, pp. 1–16.

Brasseur, P., Brankart, J.-M., Schoenauen, R., Beckers, J.-M., 1996. Seasonal temperature and salinity fields in the Mediterranean Sea: climatological analyses of a historical data set. Deep-Sea Research 43, 159–192.

Broekhuizen, N., Haeth, M.R., Hay, S.J., Gurney, W.S.C., 1995. Predicting the dynamics of the North Seas mesozooplankton. Netherlands Journal of Sea Research 33, 381–406.

Civitarese, G., Crise, A., Crispi, G., Mosetti, R., 1996. Circulation effects on nitrogen dynamics in the Ionian Sea. Oceanologica Acta 19, 609–622.

Cressman, G.P., 1959. An operational objective analysis scheme. Mon. Weather Rev. 87, 329–340.

Crise, A., et al., 1999. The Mediterranean pelagic ecosystem response to physical forcing. Progress in Oceanography 44, 219–243.

Ebenhoh, W., Kohlmeier, C., Radford, P.J., 1995. The benthic biological sub-model in the European Regional Seas Ecosystem Model. Netherlands Journal of Sea Research 33, 423–452.

Georgopoulos, D., et al., 2000. Hydrology and circulation in the Southern Cretan Sea during the CINCS experiment (May 1994–September 1995). Progress in Oceanography 46, 89–112.

Gotsis-Skretas, O., Pagou, K., Moraitou-Apostolopoulou, M., Ignatiades, L., 1999. Seasonal horizontal and vertical variability in primary production and standing stocks of phytoplankton and zooplankton in the Cretan Sea and the straits of the Cretan Arc (March 1994–January 1995). Progress in Oceanography 44, 625–649.

Ignatiades, L., 1998. The productive and optical status of the oligotrophic waters of the Southern Aegean Sea (Cretan Sea), eastern Mediterranean. Journal of Plankton Research 20 (5), 985–995.

Jaeger, L., 1976. Monatskarten des Niederschlags fur die ganze. Erde. Ber. Dtsch. Wetterdienste 18 (1839), 1–38.

Klein, P., Coste, B., 1984. Effects of wind stress variability on nutrient transport into the mixed layer. Deep-Sea Research 31, 21–37.

Krom, M.D., Kress, N., Brenner, S., 1991. Phosphorus limitation of primary productivity in the eastern Mediterranean Sea. Limnology Oceanography 36 (3), 424–432.

Kucuksezgin, F., Balci, A., Kontas, A., Altay, O., 1995. Distribution of nutrients and chlorophyll-*a* in the Aegean Sea. Oceanologica Acta 18 (3), 343–352.

Levitus, S., 1982. Climatological Atlas of the World Ocean. No. 13, NOAA, Washington.

Levy, M., Memery, L., Andre, J., 1998. Simulation of primary production and export fluxes in the north-western Mediterranean Sea. Journal of Marine Research 56, 197–238.

Lin, H.J., Nixon, S.W., Taylor, D.I., Granger, S.L., Buckley, B.A., 1996. Responses of epiphytes on eelgrass, *Zostera marina* L., to separate and combined nitrogen and phosphorus enrichment. Aquatic Botany 52, 243–258.

Mellor, G.L., 1991. An equation of state for numerical models of oceans and estuaries. Journal Atmospheric Oceanic Technology 8, 609–611.

Mellor, G.L., Yamada, T., 1982. Development of a turbulence closure model for geophysical fluid problems. Review in Geophysics and Space Physics 20, 851–875.

Moll, A., 2000. Assessment of three-dimensional physical–biological ECOHAM1 simulations by quantified validation for the North Sea with ICES and ERSEM data. ICES Journal of Marine Science 57, 1060–1068.

Patsch, J., 1994. MACADOB a model generating synthetic time series of solar radiation for the North Sea. Ber. Zentrum Meeresforsch. Klimaforsch. B 16, 1–67.

Pinazo, C., Marsaleix, P., Millet, B., Estournel, C., Vehil, R., 1996. Spatial and temporal variability of phytoplankton biomass in upwelling areas of the north-western Mediterranean: a coupled physical and biogeochemical modelling approach. Journal of Marine Systems 7, 161–191.

Psarra, S., Tselepides, A., Ignatiades, L., 2000. Primary productivity in the oligotrophic Cretan Sea (NE Mediterannean): seasonal and interannual variability. Progress in Oceanography 46, 187–204.

Richtmyer, R.D., Morton, K.W., 1994. Difference Methods for Initial-Value Problems. Krieger Publishing, Malabar, FL, 405 pp.

Smagorinsky, J., 1963. General circulation experiments with the primitive equations: I. the basic experiment. Monthly Weather Review 91, 99–164.

Solidoro, C., Crise, A., Crispi, G., Pastres, R., 1998. Local sensitivity analysis of Mediterranean sea trophic chain. In: Chan, K., Tarankola, S., Campolongo, F. (Eds.), Second International Symposium on Sensitivity Analysis of Model Output SAMO98. EUR report 17758 EN (Luxembourg), Venice, Italy, pp. 277–280.

Souvermezoglou, E., Krasakopoulou, E., Pavlidou, A., 1999. Temporal variability in oxygen and nutrient concentrations in the southern Aegean Sea and the straits of the Cretan Arc. Progress in Oceanography 44, 573–600.

Stergiou, K.I., Christou, E.D., Georgopoulos, D., Zenetos, A., Souvermezoglou, C., 1997. The hellenic seas: physics, chemistry, biology and fisheries. Oceanography and Marine Biology 35, 415–538.

Theocharis, A., Balopoulos, E., Kioroglou, S., Kontoyiannis, H., Iona, A., 1999. A synthesis of the circulation and hydrography of the South Aegean Sea and the Straits of the Cretan Arc (March 1994–January 1995). Progress in Oceanography 44, 469–509.

Thingstad, T.F., Lignell, R., 1997. Theoretical models for the control of bacterial growth rate, abundance, diversity and carbon demand. Aquatic Microbial. Ecology 13, 19–27.

Thingstad, T.F., Rassoulzadegan, F., 1995. Nutrient limitations, microbial food webs, and 'biological C-pumps': suggested interactions in a P-limited Mediterranean. Marine Ecology. Progress Series 117, 299–306.

Triantafyllou, G., Petihakis, G., Allen, J.I., 2002a. Assessing the performance of the Cretan Sea ecosystem model with the use of high frequency M3A buoy data set. Annales Geophysicae, in press.

Triantafyllou, G., Petihakis, G., Allen, J.I., Tselepides, A., 2002b. Primary production and nutrient dynamics of the Cretan Sea Ecosystem (North Eastern Mediterranean), a modelling approach. Journal of Marine Research, submitted for publication.

Tselepides, A., Polychronaki, T., 1996. Pelagic–Benthic Coupling in the Oligotrophic Cretan Sea (NE Mediterranean) IMBC, Iraklio.

Tselepides, A., Zervakis, V., Polychronaki, T., Donavaro, R., Chronis, G., 2000. Distribution of nutrients and particulate organic matter in relation to the prevailing hydrographic features of the Cretan Sea (NE Mediterranean). Progress in Oceanography 46, 113–142.

Turley, C.M., et al., 2000. Relationship between primary producers and bacteria in an oligotrophic sea—the Mediterranean and biogeochemical implications. Marine Ecology. Progress Series 193, 11–18.

Tusseau, M.H., Lancelot, C., Martin, J.M., Tassin, B., 1997. 1D coupled physical–biological model of north-western Mediterranean Sea. Deep-Sea Research. Part 2 44, 851–880.

Valiela, I., 1984. Marine Ecological Processes. Springer Advanced Texts in Life Sciences. Springer-Verlag, New York, 546 pp.

Van Wambeke, F., Christaki, U., Bianchi, M., Psarra, S., Tselepides, A., 2000. Heterotrophic bacterial production in the Cretan Sea (NE Mediterannean). Progress in Oceanography 46, 205–216.

Varela, R.A., Cruzado, A., Tintore, J., Ladona, E., 1992. Modelling the deep chlorophyll maximum: a coupled physical biological approach. Journal of Marine Research 50, 441–463.

Varela, R.A., Cruzardo, A., Gabaldon, J.E., 1995. Modelling the primary production in the North Sea using ERSEM. Netherlands Journal of Sea Research 33, 337–361.

Zakardjian, B., Prieur, L., 1994. A numerical study of primary production related to vertical turbulent diffusion with special reference to vertical motion of the phytoplankton cells in nutrient and the light field. Journal of Marine Systems 5, 267–296.

Zavatarelli, M., Barreta, J.W., Barreta-Bekker, J.G., Pinardi, N., 2000. The dynamics of the Adriatic Sea ecosystem. An idealized model study. Deep Sea Research I 47 (5), 937–970.